

Short Communication

Influence of AC interference on Crack Initiation Behavior of Pipeline Steel in High pH Solution

Min Zhu^{*}, Yongfeng Yuan, Qiang Zhang, Simin Yin, Shaoyi Guo

School of Mechanical Engineering & Automation, Zhejiang Sci-Tech University, Hangzhou 310018, PR China

*E-mail: zmii666@126.com

Received: 30 October 2019 / *Accepted:* 26 November 2018 / *Published:* 5 January 2019

Stress corrosion cracking (SCC) behavior of U-bend samples of X80 steel under AC application was investigated in high pH solution by scanning electron microscopy (SEM), macroscopic observation and polarization curves. The results show that there is a remarkable difference in corrosion morphologies of steel samples tested with or without AC current. AC application enhances the corrosion of X80 steel, and results in the occurrence of pitting corrosion. With the increasing AC current density, the corrosion degree of steel increases and the pits become more apparently. The pitting corrosion generated due to applied AC induces and facilitates the crack initiation, the greater of AC current density, the more cracks are initiated from the pits, and thus increases the SCC susceptibility of the steel.

Keywords: Pipeline steel; SCC initiation; AC application; Pitting corrosion

1. INTRODUCTION

The enhanced corrosion of metals (including pipeline steel) under AC current interference has been received increasing attention in the recent years [1-5]. Much research [6-7] indicated that the corrosion rate of metallic materials can be accelerated in the presence of AC, and localized corrosion such as pitting corrosion has been observed on the steel surface[8]. It has been reported [9-10] that corrosion pit is one of incubators of stress corrosion cracks of pipeline steel. Thus, AC may induce and facilitate the SCC failure of pipeline. To date, there has been very few research conducted on the SCC behavior of pipeline steel with AC interference. Our previous research results reported that [11], X80 steel tested under a long-term interference of AC had very high susceptibility to SCC, some SCC cracks were found to initiated from the pitting corrosion induced by AC corrosion, and AC could accelerate the

crack propagation rate of X80 pipeline steel in high pH solution[12]. In this paper, in order to study further the influence of pit corrosion induced by AC interference on crack initiation and propagation behavior, the SCC behavior of U-bend sample of X80 steel under a long-term effect of AC application is investigated in high pH solution by the immersion test. After the test, the crack initiation behavior is analyzed by scanning electron microscope (SEM).

2. EXPERIMENTAL

The specimens were cut from hot-rolled plate of API X80 pipeline steel. The chemical composition of the steel is (wt%): C 0.070, Si 0.216, Mn 1.80, P 0.0137, S 0.0009, Mo 0.182, Cr 0.266, Cu 0.221, Ni 0.168, Nb 0.105, Al 0.026, Ti 0.013, V 0.001, N 0.003 and Fe balance. The microstructure of the steel is mainly composed of polygonal ferrite, acicular ferrite and a number of granular bainites (Fig.1).

As illustrated in Fig.2a, the U-bend specimens were prepared according to GB T 15970 specification. Prior to the test, the surface of the U-bend specimen was ground to 2000 grit emery paper along the tensile direction, then degreased with acetone, followed by cleaning with distilled water and finally dried in air. The specimens were coated with a silicone, leaving an exposure area of 2 cm² as the working surface. According to the design thinking of the test, the exposure area was the part of high ridge of the specimen, i.e., the region of the maximum strain, as shown in Fig.2b. In the laboratory test, the carbonate/bicarbonate solution (0.5 M Na₂CO₃+1 M NaHCO₃) was widely used as the simulated solution for high pH SCC of buried pipeline steels. The pH of the solution was 9.32. The U-bend specimen was immersed in the solution, and AC current density in the range of 0-200 A/m² was applied to the sample. During the whole process of immersion test for 30 days, the sine wave AC with a frequency of 50 Hz was applied between the specimen and graphite electrode, meanwhile, the sample was conducted at a polarized potential of -580 mV (vs. SCE). The potential applied to the specimen was in the middle of the potential range causing IGSCC [13]. The sample was maintained at the potential via a PS-12 potentiostat and a three-electrode system, where the U-bend sample was used as the working electrode, a platinum plate as counter electrode and a saturated calomel electrode (SCE) as reference electrode. The test was performed at ambient temperature (~22 °C) and repeated at least three times. After the test, the corrosion morphology of high ridge region of the specimens at various AC current densities was analyzed by scanning electron microscopy (figure 6) (SEM), macroscopic observation (figure 3-4) and 3D imaging (figure 5).

Moreover, potentiodynamic polarization curve of the coated U-bend specimen of X80 steel (under strain state) was tested on PARSTAT2273 electrochemical workstation with a three-electrode cell system. The AC corrosion experimental set-up for electrochemical measurement was in line with our previous researches [11,14]. The superimposed AC current density range was the same as the above immersion test. Before the test, the U-bend specimen was immersed in the solution for 1h to reach a steady state. Polarization curves were performed at the potential range of -1.0~1.2V (vs.SCE) with a scan rate of 0.5 mV/s.

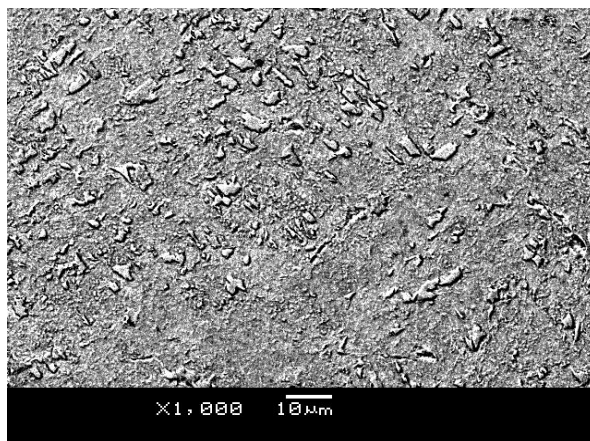


Figure 1. Metallograph of X80 pipeline steel

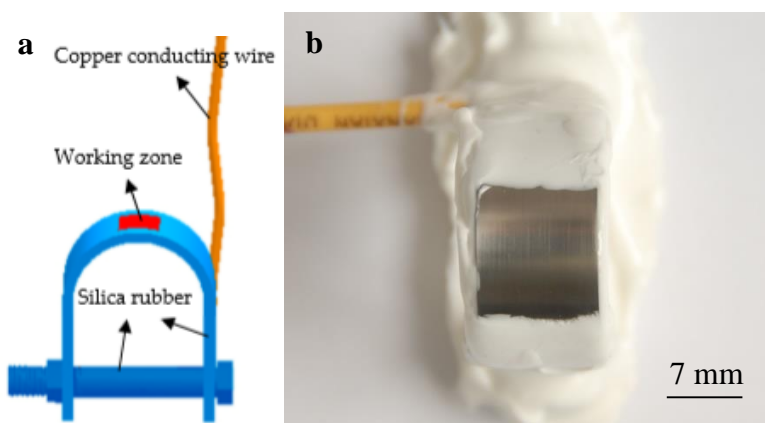


Figure 2. U-bend sample (a) sketch map, (b) coated specimen

3. RESULTS

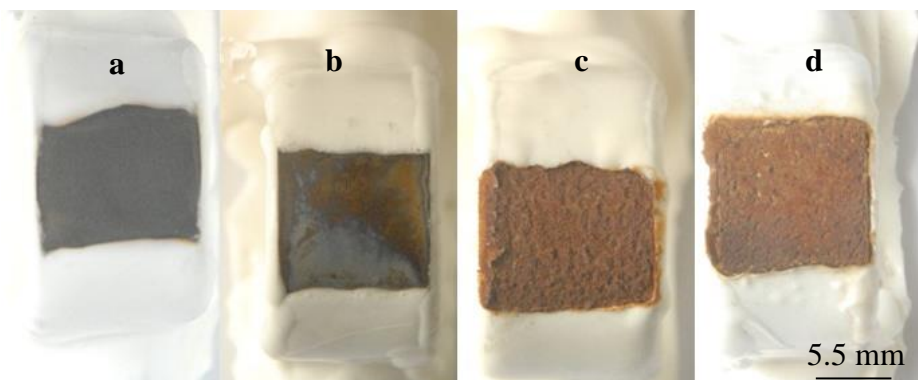


Figure 3. Macro-morphologies of U-bend sample of X80 steel at various AC current densities in carbonate/bicarbonate solution (a) without AC, (b) 30 A/m², (c) 100 A/m², (d) 200 A/m².

Fig.3 shows the macro-morphologies of U-bend sample of X80 steel at various AC current densities. At the absence of AC superimposition, the steel surface is covered by black corrosion product,

and the corrosion degree of specimen is relatively slight. Compared with that without the presence of AC application, AC enhances the corrosion of the steel. And the corrosion degree of steel sample becomes severely with the increased AC current density. When the steel specimen is applied at a low AC current density of 30 A/m^2 , few tan and light blue corrosion products are formed on the surface of steel specimen, exhibiting a slight corrosion feature. With a further increase of AC current density to 100 A/m^2 and 200 A/m^2 , the serious corrosion of the steel is observed, and there are a large quantity of yellow-brown corrosion products distributed on the specimen surface.

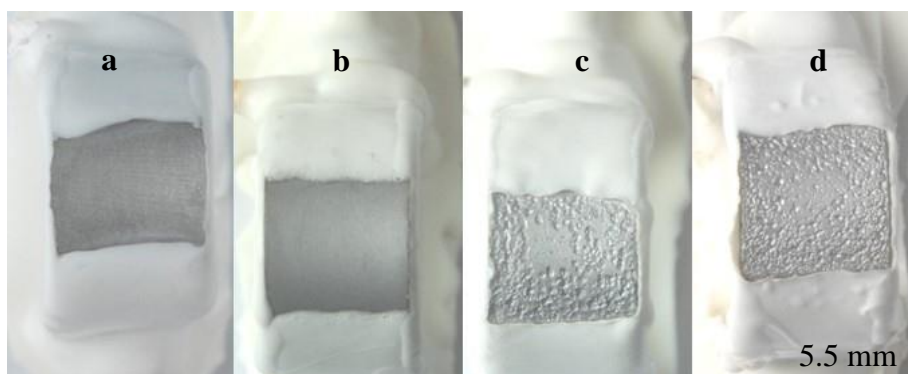


Figure 4. Macro-morphologies of U-bend sample of X80 steel at various AC current densities in carbonate/bicarbonate solution following the removal of corrosion product (a) without AC, (b) 30 A/m^2 , (c) 100 A/m^2 , (d) 200 A/m^2 .

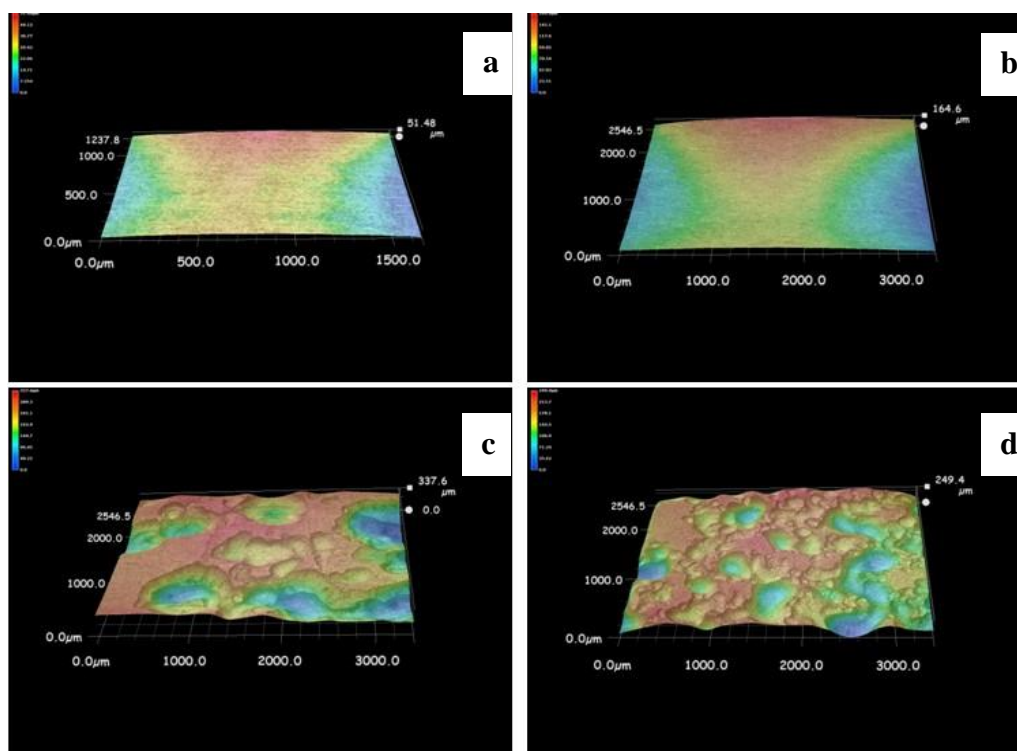


Figure 5. 3D imaging of corrosion morphologies of U-bend sample of X80 steel at various AC current densities in carbonate/bicarbonate solution following the removal of corrosion product (a) without AC, (b) 30 A/m^2 , (c) 100 A/m^2 , (d) 200 A/m^2 .

Fig.4 shows the macro-morphologies of U-bend sample of X80 steel at various AC current densities following the removal of corrosion product. It is clearly shown that there is a significant difference in the corrosion morphologies of specimens with or without AC application. As Fig.4a reveals that, when AC current is absent, no obvious pits are observed on the surface of sample. Under the macroscopic observation, the morphology feature of specimen at 30 A/m² is analogous to that at the absence of AC. With the increasing of AC current density, the pits become more apparently, and the pit number greatly increases, resulting in an intensive distribution on the whole surface of steel sample.

Figure 5 shows 3D imaging of corrosion morphologies of U-bend sample of X80 steel at various AC current densities following the removal of corrosion product. The images reveal that the increasing of AC current density obviously promotes corrosion degree of the steel, and accelerates the occurrence of localized corrosion. Especially at high AC current densities of 100 A/m² and 200 A/m², the severe pits can be observed on the surface of U-bend samples, and some corrosion pits are very large and deep. Furthermore, some small-sized pits fuse together and form a larger-sized pit. In contrast, the degree of pit corrosion on the surface of the samples tested without AC application or at the low AC current density of 30 A/m² is relatively slighter.

The above corrosion morphologies (Fig. 3-5) are based on macroscopic or low magnification observation. Fig.6 shows the micro-morphologies of U-bend sample of X80 steel at various AC current densities following the removal of corrosion product. There is a remarkable difference in micro-corrosion morphologies of steel samples tested with or without AC current. It is seen from Fig.6a that, the cracks are intergranular, and there is an apparent phenomenon of grains removal, which are identical with the feature of IGSCC fracture. In contrast, under AC application, there are obvious pits formed on the specimens at various AC current densities. With the increasing of AC current density, the number and size of pits increase significantly. In particular, the small pits are connected into the big one, even at 30 A/m². Moreover, Fig.6b, c and d shows that the SCC cracks are initiated from the pits. In addition, the greater AC current density, the more cracks are initiated from the pits. This is verified that the pitting corrosion induced by AC facilitates the crack initiation [11], which greatly increases the SCC susceptibility of the steel, and accelerates the crack propagation at some extent [12]. Furthermore, the significant difference in micro-corrosion morphology of specimens demonstrates that the SCC mechanism of steels tested with or without AC in high pH solution is remarkably different [11].

Under the condition of imposed AC, the generated H atom [11] would diffuse into the steel, and hydrogen enrichment could easily occur at the region of stress concentration, such as the pitting corrosion. In addition, solution acidification or the decrease of pH due to the autocatalytic acidification effect generally occurs at the bottom of the pits. Thus, the pits caused by AC could easily induce and facilitate the initiation of cracks (Fig.6).

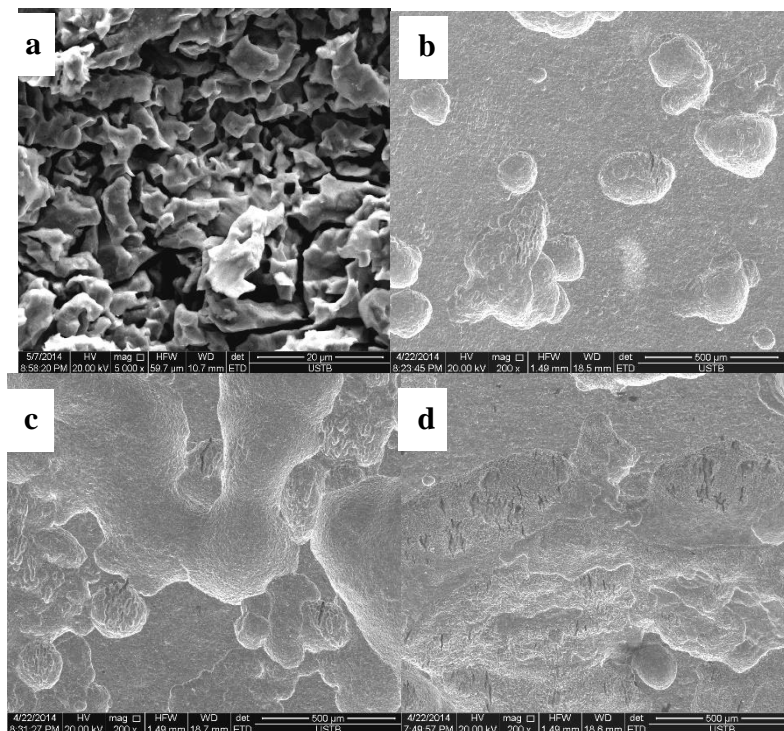


Figure 6. Micro-morphologies of U-bend sample of X80 steel at various AC current densities in carbonate/bicarbonate solution following the removal of corrosion product (a) without AC, (b) 30 A/m², (c) 100 A/m², (d) 200 A/m².

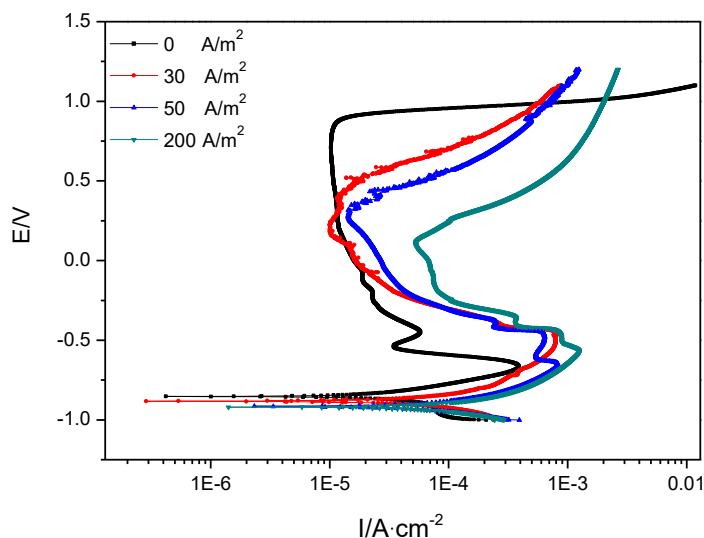


Figure 7. Polarization curves of U-bend sample of X80 steel at various AC current densities in carbonate/bicarbonate solution

Fig.7 shows the polarization curves of U-bend sample of X80 steel at various AC current densities. Superimposed AC significantly reduces the passivity of steel under the strain state. AC application mainly affects the anode curves, which increases the passive current density (i_p) and shifts the critical pit potential (E_b) negatively. Table.1 reveals that imposed AC greatly promotes the i_p value, i.e. AC application accelerates the corrosion rate of steel, especially at the high current density of 200

A/m². Table.1 also shows that AC shifts E_b value negatively at a great extent, which indicates that pitting corrosion could be easily formed on the sample surface, even at the low AC current density of 30 A/m². This can be verified in Fig.6. It is well known that pits corrosion could accelerate the initiation of crack. As shown in Fig.6, the pitting corrosion generated by applied AC could increases SCC susceptibility. At high pH solution, the SCC behavior of pipeline steel is related to the rupture of passive film [15-16]. The curve change in Figure 7 demonstrates that AC could decrease the film stability, which could accelerate the SCC process.

Table 1. Fitted electrochemical parameter of U-bend sample of X80 steel at various AC current densities in carbonate/bicarbonate solution

i _{AC} (A·m ⁻²)	i _p (10 ⁻⁵ A·cm ⁻²)	E _B (V)
0	1.038	0.855
30	1.258	0.403
50	1.447	0.312
200	5.666	0.112

4. CONCLUSIONS

AC interference obviously promotes corrosion degree of U-bend sample of X80 pipeline steel, and accelerates the occurrence of pitting corrosion. With the increasing AC current density, the corrosion degree of steel increases and the pits become more apparently. Pitting corrosion generated by applied AC induces and facilitates the crack initiation, the greater of AC current density, the more cracks are initiated from the pits, and thus increases the SCC susceptibility of the steel.

ACKNOWLEDGEMENTS

This work was support by the National Natural Science Foundation of China, the Natural Science Foundation of Zhejiang province (No. LY18E010004), and the National R&D Infrastructure and Facility Development Program of China (No. 2005DKA10400).

References

1. S.B. Lalvani and G. Zhang, *Corros. Sci.*, 37(1995)1567.
2. A. B renna, S. Beretta, F. Bolzoni, M.P. Pedefferri and M. Ormellese, *Constr. Build. Mater.*, 137(2017) 76.
3. Y.B.Guo,T.Meng, D.G.Wang,H.Tan and R.Y.He, *Eng.Fail.Analy.*, 78(2017)87.
4. K.K.Tang, *Cement concrete Res.*, 100(2017)445.
5. Nagat M. K. Abdel-Gawad, Adel Z. El Dein and M. Magdy, *Electr. Pow. Syst. Res.*, 127(2015)297
6. J.L. Wendt and D.T. Chin, *Corros. Sci.*, 25(1985)889.
7. A.Q. Fu and Y.F. Cheng, *Corros. Sci.*, 52(2010)612.
8. Y.B. Guo, H. Tan, D.G. Wang and T. Meng, *Anti-Corros. Method.M.*, 64(2017)599.
9. B.G. Van, W. Chen and R. Rogge, *Acta. Mater.*, 55(2007)29.
10. W. Chen, F. King and E. Vokes, *Corrosion*, 58(2002)267.
11. M. Zhu, C.W. Du, X.G. Li, Z.Y. Liu, H. Li and D.W. Zhang, *Corros. Sci.*, 87(2014)224.

12. M. Zhu, G. F. Ou, H.Z. Jin, C.W. Du, X.G. Li and Z.Y. Liu, *J. Mater. Eng. Perform.*, 24(2015) 2422.
13. Z. F. Wang and A. Atrens, *Metall. Mater. Trans. A*, 27(1996)2686.
14. M. Zhu, C.W. Du, X.G. Li, Z.Y. Liu, S.R. Wang, J.K. Li and D.W. Zhang, *Electrochim. Acta*, 117(2014) 351.
15. R.N. Parkins, *Corrosion*, 52(1996)363.
16. A. Mustapha, E.A. Charles and D. Hardie, *Corros. Sci.*, 54(2012)5.

© 2019 The Authors. Published by ESG (www.electrochemsci.org). This article is an open access article distributed under the terms and conditions of the Creative Commons Attribution license (<http://creativecommons.org/licenses/by/4.0/>).